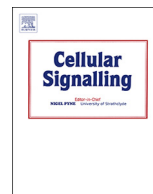




ELSEVIER

Contents lists available at ScienceDirect

## Cellular Signalling

journal homepage: [www.elsevier.com/locate/cellsig](http://www.elsevier.com/locate/cellsig)

## A novel Rhein derivative: Activation of Rac1/NADPH pathway enhances sensitivity of nasopharyngeal carcinoma cells to radiotherapy

Zhengying Su<sup>a,1</sup>, Zhaoquan Li<sup>a,1</sup>, Chunmiao Wang<sup>a</sup>, Wei Tian<sup>a</sup>, Fu Lan<sup>a</sup>, Dandan Liang<sup>a</sup>, Junying Li<sup>a</sup>, Danrong Li<sup>b,\*</sup>, Huaxin Hou<sup>a,\*</sup>

<sup>a</sup> College of Pharmacy, Guangxi Medical University, Nanning, Guangxi 530021, China

<sup>b</sup> Guangxi Institute for Cancer Research, Nanning, Guangxi 530021, China



## ARTICLE INFO

## Keywords:

Nasopharyngeal carcinoma  
Rhein derivative  
Radiosensitizers  
Molecular docking  
Rac1/NADPH signaling pathway

## ABSTRACT

Radiation resistance and recurrent have become the major factors resulting in poor prognosis in the clinical treatment of patients with nasopharyngeal carcinoma (NPC). New strategies to enhance the efficacy of radiotherapy have been focused on the development of radiosensitizers and searching for directly targets that modulated tumor radiosensitivity. A novel potential radiosensitizer 1,8-Dihydroxy – 3-(2'-(4'-methylpiperazin-1'-yl) ethyl-9,10-anthraquinone – 3-carboxylate (RP-4) was designed and synthesized based on molecular docking technology, which was expected to regulate the radiosensitivity of tumor cells through targeting Rac1. In order to assess the radiosensitization activity of RP-4 on NPC cells, the highly differentiated CNE1 and poorly differentiated CNE2 cells NPC lines were employed. According to the results, RP-4 showed higher binding affinity toward the interaction with Rac1 than lead compounds. We found that RP-4 could inhibit cell viability and proliferation in CNE1 and CNE2 cells and significantly induced apoptosis after non-toxic concentration of RP-4 combined with 2Gy irradiation. RP-4 could effectively modulated the radiosensitivity both CNE1 cells and CNE2 cells through activating Rac1/NADPH signaling pathway and its downstream JNK/AP-1 pathway. What's more, Rac1/NADPH signaling pathway were significantly activated in Rac1-overexpressed CNE1 and CNE2 cells after treated with RP-4. Taken together, Rac1 and its downstream pathway may probably be the direct targets of RP-4 in regulating radiosensitivity of NPC cells, our finding provided a novel strategy for the development of therapeutic agents in response to tumorous radiation resistance.

### 1. Introduction

According to the epidemiological investigation, nasopharyngeal carcinoma (NPC) has an ethnic and geographical distribution in southern China, where the morbidity is 25-fold higher than other countries [1]. Radiation therapy is considered to be a first-line therapy modality for most of the cancers including breast cancer, head and neck cancer, and many others [2]. However there is no specific selectivity between normal tissues and tumor cells when patients receiving radiotherapy, and what makes matter worse is that the majority of tumors cells are remaining in a hypoxic condition which consequently leading to the resistance to radiation [3]. Therefore, it is really an urgent to develop potent strategies to improve the radiosensitivity for treatments. Recently, the research and development of radiosensitizer targeted to DNA damage repair was emerging [4]. For example, the nitro-compound is a classical electron-affinic radiosensitizers, however,

the serious side effects of which makes it difficult to achieve a wide range of applications in clinic [3].

In our previous study, the Rac1 protein was discovered to be a promising mitochondrial target in the radiosensitization process of GXHSAQ-1 (1, 8-dihydroxy-3-acetyl-6-methyl-9, 10 anthraquinone, which contains an anthraquinone planer basic skeleton) by using the method of proteomic approach with an isobaric tag for relative and absolute quantitation [5]. We also reported that one of the anthraquinone compounds Rhein showed significant radiosensitization activity on NPC cells and possessed strong binding affinity with Rac1 [6]. Rac1 is a member of Rho family of GTPases including Cdc42 and RhoA. It closely associates with many cell biological functions, such as cell trafficking, actin polymerization, gene transcription, and cell proliferation [7,8]. It has been reported that the small GTPase Rac1 participates in regulating the activation of NADPH oxidase complex which resulting in intracellular superoxide production, such as an increase of

\* Corresponding author at: Shuangyong Road No. 22, Guangxi Medical University, Nanning, Guangxi 530021, China.

E-mail address: [13367805966@163.com](mailto:13367805966@163.com) (H. Hou).

<sup>1</sup> These authors contributed equally to this work.

<https://doi.org/10.1016/j.cellsig.2018.11.015>

Received 18 August 2018; Received in revised form 4 November 2018; Accepted 16 November 2018

Available online 18 November 2018

0898-6568/ © 2018 Elsevier Inc. All rights reserved.

reactive oxygen species [3,9,10]. The induced generation of ROS production was considered to result in DNA damage followed by the apoptosis mediated by mitochondrial intrinsic pathways [11]. We previously identified that irradiation could significantly activate Rac1, NADPH oxidase and then increase ROS production in NPC CNE1 cells, thereby promoting the apoptosis of the cells [12]. Obviously, the activation of Rac1/NADPH signaling pathway was strongly linked to the radiation sensitivity of nasopharyngeal carcinoma. Inspired by our discovery, we conceived a series of ideas to design and research new radiotherapy sensitization agents specifically directing at this key target and signaling pathway. Previous studies have identified the radiotherapy sensitization activity of GXHSWAQ-1, whereas the poor water solubility become a big obstacle in practical application. In order to obtain a novel radiosensitizer with an improved water solubility that strongly targeting at Rac1 protein, we conducted a drug design through molecular docking technique based on the anthraquinone compound Rhein. And a novel Rhein derivative, 1,8-Dihydroxy-3-(2'-(4"-methylpiperazin-1"-yl) ethyl)-9,10-anthraquinone-3-carboxylate (RP-4 for short) was designed and synthesized by introducing N-(2-Hydroxyethyl) piperazine to Rhein without altering the anthraquinone nuclear structure.

In this work, we devoted to explore whether the radiotherapy sensitization effects of new compound RP-4 on NPC cells was targeting Rac1 and mediating Rac1/NADPH pathway and its downstream JNK/AP-1 pathway during radiotherapy treatment using different differentiation levels of NPC cell models. In addition, we expected to obtain desirable radiosensitizers based on these key targets of radiotherapy sensitization through structure modification on anthraquinone compound. We believed that the results we reported would provide new strategies for the development design of radiotherapy sensitization agent with an anthraquinone nucleus structure.

## 2. Material and method

### 2.1. Chemistry

#### 2.1.1. Synthesis route

**2.1.1.1. Synthesis of 1,8-Dihydroxy-3-(2'-(bromoethyl)9,10-anthraquinone-3-carboxylate (1).** Rhein (248.2 mg, 1 mmol), potassium carbonate (1 g, 7.24 mmol) suspended in anhydrous dimethyl formamide (DMF, 10 mL) in a dry round bottom flask and warmed to 60 °C. Then 1,2-dibromoethane (432 µL, 5 mmol) was added and stirred at 60 °C for 1 h under N<sub>2</sub>. TLC (petroleum ether: ethyl acetate = 4: 1) showed complete consumption of the starting material, the mixture's color turned from yellow to deep purple. The mixture was poured into ice water (50 mL) and acidified with HCl (2 M). The solution color changed to yellow and precipitation was observed. The precipitation was filtered to give crud product as an orange solid. The residue was purified by column chromatography on silica gel (petroleum ether/ethyl acetate 8:1) to give the desired product as an orange-red solid (**Compound 1**).

**2.1.1.2. Synthesis of 1,8-Dihydroxy-3-(2'-(4"-methylpiperazin-1"-yl) ethyl)-9,10-anthraquinone-3-carboxylate (compound 2, RP-4).** Compound 1 (117.4 mg, 0.3 mmol) was dissolved in anhydrous 1,4-dioxane (5 mL), then N-methylpiperazine (166 µL, 1.5 mmol) was added and stirred at 85 °C for 2 h under N<sub>2</sub>. Removed all solvent in vacuum, the residue was purified by column chromatography on silica gel (Dichloromethane/Methanol 30:1) and recrystallization from dichloromethane+petroleum ether to give the desired product as a yellow solid. The structure of compound was confirmed by IR spectra using Perkin-Elmer 1600 series FTIR spectrometer (USA). <sup>1</sup>H- and <sup>13</sup>C-NMR spectra were run on a Bruker 300 Ultrashield NMR (Switzerland) at 300 and 75.5 MHz, respectively, using CDCl<sub>3</sub> (Merck) as solvent. All the reagents purchased from Aladdin Inc. (Ontario, CA 91761, USA).

### 2.2. Molecular docking

The interaction of chemical compounds with macromolecule Rac1 was employed by (Molecule Operating Environment) MOE 2008, a software package for molecular docking study.

#### 2.2.1. Preparation of the ligands

The 3D structures of GXHSWAQ-1 and RP-4 were generated using MOE 2008 builder, and subjected to energy minimization using the Merck Molecular Force Field 94 × (MMFF94x), which was more preferable for organic molecules [13]. Hydrogen and partial charges were calculated by protonation 3D function in MOE [14]. The structure files of the ligands were saved as PDB format for further docking study.

#### 2.2.2. Preparation of the macromolecule

The crystal structures of the protein Rac1 (PDB code: 1I4D) was downloaded at the website of Protein Data Bank (<http://www.pdb.org>). The non-target proteins inside the macromolecule were manually removed from the structure coordinate. The energy optimization of the receptor was employed with the Amber89 force field which was different with the preparation of ligands [15]. In addition, the processing of hydrogen and partial charges was absolutely the same with the ligands.

#### 2.2.3. Molecular docking procedure

The active site of the receptor was predicted using Site Finder of MOE, a method to comprehensively evaluate the pocket shape, size and the number of hydrophobic residues, and select the optimal pocket as active site for docking program. The ligand molecules were docked in the active site of Rac1, the default London dG scoring function of MOE was employed to rank the binding affinity of the ligand and the receptor. The docking result was described as the binding energy (London dG values) and most reasonable conformation of the ligand interaction with receptor.

### 2.3. Biologic evaluation

#### 2.3.1. Cell culture and groups

The highly differentiated human NPC CNE1 cell line and poorly differentiated human NPC CNE2 cell line were kindly provided by Guangxi Cancer Institute (Nanning, China). The two lines of differently biological human NPC cells were applied as the experimental cell models.

Rac1 was separately knocked down by shRNA in both CNE1 and CNE2 cells which were named as CNE1-Rac1(-) and CNE2-Rac1(-) cells, while the overexpressed Rac1 cell lines were named as CNE1-Rac1(+) and CNE2-Rac1(+) cells. All of the above cell lines were cultured in RPMI 1640 medium (Gibco) with 10% fetal calf serum (Gibco), penicillin (50 unit·mL<sup>-1</sup>) and streptomycin (50 µg·mL<sup>-1</sup>) and were kept in a cell incubator at 37 °C with humid atmosphere at 5% CO<sub>2</sub>.

In order to explore the relationship between RP-4 and radiotherapy sensitization, the NPC CNE1 and CNE2 cells were divided into four groups, they were control which was untreated with irradiation or RP-4, 2Gy irradiation treatment group, RP-4 treatment group and 2Gy irradiation combined with RP-4 treatment group. Both the 2Gy irradiation group and RP-4 combined 2Gy irradiation groups were irradiated at room temperature using a Siemens linear accelerator (Siemens, Concord, CA) at a dose rate of 266 cGy/min.

#### 2.3.2. Determination of cell viability

Cell viability was determined by MTT assay. The logarithmic phase of CNE1 and CNE2 cells were chosen as the experimental objects. The cells were digested by trypsin and plated in 0.1 mL of RPMI 1640 medium at a density of 5000 cells in 96-well plates. After attaching for 24 h, the cells were exposed to RP-4 at the final concentration of 0, 6.25, 12.5, 25, 50 and 100 µg·mL<sup>-1</sup>. The cells were terminated from the

exposure after another 24 h by incubating with 20  $\mu\text{L}$  MTT (0.5 mg/mL; Sigma) at 37 °C for 4 h in the dark. The formazan crystal was dissolved by 100  $\mu\text{L}$  DMSO, and the absorbance values of which were read at 492 nm using a Synergy H1 multimode plate reader (BioTek). The viability of the cells was scored by the percentage of absorbance relative to control.

### 2.3.3. Determine the activity of the intracellular NADPH oxidase

The activity of NADPH oxidase of CNE1 and CNE2 cells was measured by nitroblue tetrazolium assay. Briefly,  $5 \times 10^5$  cells in 2 mL suspension were seeded in 6-well plates. After adherently growing for 24 h, the cells were dealt with or without RP-4 and irradiation. Then cells of each group were harvested in the microcentrifuge tube, washed with PBS for three times and incubated with 200  $\mu\text{L}$  nitroblue tetrazolium (NBT) solution (1 mg·mL<sup>-1</sup>, Solarbio, Beijing, China) for 20 min at 37 °C. 200  $\mu\text{L}$  1 mol·L<sup>-1</sup> HCl was added to terminate the reaction on the ice for 5 min. Centrifuged the reaction mixture to abandon the supernatant at 1200 g for 10 min. 100  $\mu\text{L}$  DMSO was added to dissolve the triphenylmethyl crystallization, and the absorbance value of each sample was read at 560 nm.

### 2.3.4. Measurement of intracellular ROS

The logarithmic phase of CNE1 and CNE2 cells were seeded in 6-well plates at the density of  $1 \times 10^5$  cells mL<sup>-1</sup> with triplicate for each group. After different treatments, the cells were centrifuged to get rid of the medium and washed by PBS at least twice. The collected cells were incubated with the oxidant-sensitive dye 2,7-dichlorodihydrofluorescein diacetate (DCFH-DA, cat. no. D6883; Sigma-Aldrich LLC, St. Louis, MO) at 37 °C for 20 min in the darkness. The cells of negative control were suspended in 400  $\mu\text{L}$  PBS instead of incubating with DCFH-DA. After the incubation, the cells except of negative control, were centrifuged to abandon the supernatant, washed and resuspended with PBS. Finally, all the samples were analyzed by flow cytometry technology to detect the intracellular ROS production (BD Biosciences).

### 2.3.5. Apoptosis assay

The apoptosis rates of CNE1 and CNE2 cells were performed by flow cytometry.  $2 \times 10^5$  cells were suspended in 2 mL of medium and were seeded in 6-well plates for four groups with triplicate. After each group underwent different treatments, the cultural media was changed by complete medium for further incubation for 24 h. The cells were harvested with trypsin and suspended in the binding buffer at the density of  $1 \times 10^5$  cells mL<sup>-1</sup>, then dyed with Annexin V-PE/7-AAD apoptosis detection kit (cat. no. V13241; Thermo Fisher Scientific). 5  $\mu\text{L}$  Annexin V and 1  $\mu\text{L}$  7-AAD were added to cell suspension and incubated at room temperature for 15 min in the darkness. After the incubation, another 400  $\mu\text{L}$  binding buffer was added to each sample, and then analyzed by flow cytometry.

### 2.3.6. Western blotting analysis

The whole lysates of each group were collected to obtain the protein samples for Western blot analysis. The concentration of the total protein was quantified by BCA protein assay kit. Protein samples were separated on 10% SDS-PAGE gels, and electrophoresed in Tris-glycine buffer at a constant voltage of 100 V. The protein samples were subjected to transferring from the gel to nitrocellulose membrane (Millipore, MA, USA) at a constant voltage of 100 V for 1.5 h. The membranes were blocked with 5% skim milk for 2 h at room temperature, followed by incubation of primary antibodies at 4 °C over night. The following primary antibodies were used, including GAPDH (Geneson, GP0003, Guangzhou, China), Rac1, p67<sup>phox</sup>, p47<sup>phox</sup>, p38, phosphorylate-p38 (P-P38), AP-1, phosphorylate-AP-1 (P-AP-1), JNK1/2, and phosphorylate-JNK (P-JNK) (Abcam, Cambridge, UK). The membranes were washed with PBS for three times, and then incubated with secondary antibody (Anti-Rabbit IgG (H + L), DyLight 800 labeled or Anti-Mouse IgG (H + L) HSA, DyLight 680 labeled) for 1.5 h at room temperature in

the darkness. Then the membranes were washed with PBST for three times in dark and the protein blots were visualized using the Odyssey Infrared Imaging System (Odyssey, LI-COR biosciences, Bad Homburg, Germany). The intensity of the bands were quantitatively determined by ImageJ software. GAPDH was used as loading control. The relative protein expression was described as the gray value of the target protein relative to the internal reference protein of GAPDH, and the relative protein expression rates of different groups were compared with control.

### 2.3.7. Rac1-GST pull-down assay

The activation of Rac1 were performed by pull-down assay and Western blot described as before [12]. The CNE1 and CNE2 cells after different treatments were lysed by  $1 \times$  magnesium containing lysis buffer (MLB) for 5 min on the ice to obtain the cell lysates. 2000  $\mu\text{g}$  protein samples of each group were quantitatively contained in 500  $\mu\text{L}$  cell lysates which were determined by BCA protein assay kit. Cell lysates treated with GTP $\gamma$ S to activate endogenous Rac1 and compared to lysates treated with GDP to inactivate the small GTPase. Then 10  $\mu\text{L}$  (10  $\mu\text{g}$ ) of GST PAK1 PBD beads (glutathione S-transferase (GST), p21-activated kinase 1 (PAK1), protein-binding domain (PDB)), Magnetic Beads; EMD Millipore, Billerica, MA) was added in the 500  $\mu\text{L}$  cell lysate for incubation of 1 h at 4 °C, during which gently blend the lysates every 10 min. The beads was then washed with  $1 \times$  MLB for three times. At last, 24  $\mu\text{L}$  ultrapure water, 16  $\mu\text{L}$  loading buffer and 2  $\mu\text{L}$   $\beta$ -mercaptoethanol (BME) were added in each sample, instantaneous centrifuged a few seconds and bathed in the boiling water for 5 min. The PAK1 PBD beads and Rac1 protein complexes of every sample was detected by Western blot and the protein bands were visualized using the Odyssey Infrared Imaging System.

## 2.4. Statistical analysis

All the data of the experiments represented for three individual repeated experiments ( $n = 3$ ) which were shown as mean  $\pm$  standard deviation (SD). One-way ANOVA was used to analyze the statistical differences among multiple groups, followed by L-SD *t*-test for pairwise comparison. *p*-value < 0.05 was considered to be statistically significant. Figures were obtained by the Statistical Analysis System (GraphPad Prism 5, GraphPad Software, Inc., San Diego, CA).

## 3. Result

### 3.1. Chemistry properties of RP-4

The melting point of RP-4 is 144–146 °C. The structure of RP-4 was identified as 1,8-Dihydroxy-3-(2'-(4"-methylpiperazin-1"-yl) ethyl-9,10-anthraquinone - 3- carboxylate. Complete IR, <sup>1</sup>H NMR (CDCl<sub>3</sub>) and <sup>13</sup>C NMR(CDCl<sub>3</sub>) data of RP-4 were listed in follows, IR (KBr, cm<sup>-1</sup>): 3188, 3088, 2973, 2931, 2801, 2744, 1718, 1673, 1626, 1604, 1569, 1468, 1450, 1405, 1383, 1354, 1287, 1273, 1259, 1235, 1199, 1151, 1089, 1013, 763, 747, 698, 594. <sup>1</sup>H NMR (500 MHz, CDCl<sub>3</sub>)  $\delta$  11.97 (s, 2H), 8.39 (s, 1H), 7.92 (s, 1H), 7.86 (d, *J* = 7.5 Hz, 1H), 7.72 (s, 1H), 7.33 (d, *J* = 8.4 Hz, 1H), 4.51 (t, *J* = 5.9 Hz, 2H), 2.82 (t, *J* = 5.9 Hz, 2H), 2.63 (s, 4H), 2.45 (s, 4H), 2.30 (s, 3H). <sup>13</sup>C NMR (126 MHz, CDCl<sub>3</sub>)  $\delta$  192.80, 180.91, 164.31, 162.80, 162.39, 138.00, 137.76, 133.89, 133.48, 125.35, 124.91, 120.39, 120.27, 118.24, 115.83, 63.42, 56.47, 55.06, 53.36, 46.00. Water solubility of RP-4 was greatly improved compared with GXHSAQ-1 and the liposome–water partition coefficients (expressed as LogP) of RP-4 predicted by Chem Bio Draw Ultra was 1.22, which was significantly lower than GXHSAQ-1 (LogP = 1.71).

### 3.2. Rac1 expression level of two NPC cell lines

In our previous study, the Rac1 protein was discovered to be a

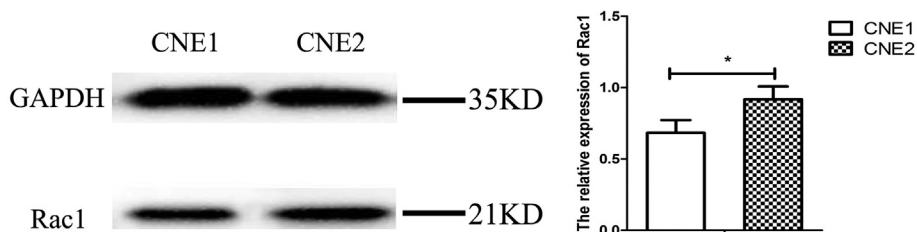


**Fig. 1.** The different expression level of Rac1 between the two nasopharyngeal carcinoma cell lines. The protein expression level was measured by western blotting. GAPDH was used for loading control. All the data represented for three individual repeated experiments.

\*P < 0.05 for Rac1 expression in CNE1 cells vs. CNE2 cells.

promising mitochondrial target in the radiosensitization process of GXHWSAQ-1. Rac1 is known to closely relate to the radiosensitization [12]. The expression of Rac1 in both CNE1 and CNE2 cells was detected by Western blotting analysis, it was clear from the results that a higher expression of Rac1 was detected in the poorly differentiated CNE2 cells compared with CNE1 cells, which suggested that CNE2 cells was more sensitive to radiotherapy (Fig. 1).

### 3.3. Molecular docking result

Molecular docking was widely applied to predict the interaction of the compounds and target proteins. In order to study the binding affinity of Rac1 with GXHWSAQ-1 and RP-4, molecular docking was conducted using MOE 2008. The docking energy was considered to be better when its London dG value was more negative than  $-7.5$  kcal/mol [16], and the more negative London dG values predicted higher binding affinity between targets and ligands. Among different molecular interactions, hydrogen bond was considered to be the major molecular interaction force which contributed great to stabilize the receptor-ligand complexes. Besides, compared with side chain hydrogen bond interaction, the backbone hydrogen bond was superior in stabilizing the complexes. According to the docking conformations of the two compounds, both GXHWSAQ-1 and RP-4 interacted with Rac1 in a similar pattern and embed within Rac1 binding pocket (Fig. 2c). Two hydroxyl groups of GXHWSAQ-1 on anthraquinone ring participated in forming two side chain hydrogen bond interactions with amino residue ThrC17 of Rac1, meanwhile creating a stable chelation interaction with magnesium ion. (Fig. 2a) Similarly, both ThrC17 and magnesium ion were involved in forming chelation interactions with one of

**Table 1**

Calculated London dG scoring of the ligand docking with Rac1.

Ligand	London dG (kcal/mol)
GXHWSAQ-1	-15.5737
RP-4	-19.9711

the hydroxyl group of RP-4 on its anthraquinone ring. In addition, the sidechain hydrogen bond interactions was found to form with LysC116, while a backbone hydrogen bond interactions was formed between the residue GlyC15 and RP-4, which greatly enhanced the binding affinity of RP-4 and Rac1 (Fig. 2b). The docking results showed that RP-4 possessed higher binding affinity toward the interaction with Rac1 than GXHWSAQ-1 (shown as Table 1), which suggested a rational structure modification. Inspired by the docking simulation results, we hypothesized whether the high binding affinity predicted desirable pharmacological activity, therefore, we next conducted a series of in vitro bioactivity experiments to verified the interaction of RP-4 with Rac1, and evaluate the possibility of RP-4 to be a radiosensitizer by targeting Rac1 protein.

### 3.4. The inhibitory effects of RP-4 on the growth of NPC CNE1 and CNE2 cells

In order to assess the biological activity of RP-4 on NPC cells, the different differentiation levels of NPC CNE1 and CNE2 cell lines were employed. The viability of NPC CNE1 and CNE2 cells after treatment with different concentrations of RP-4 were detected by MTT assay. The

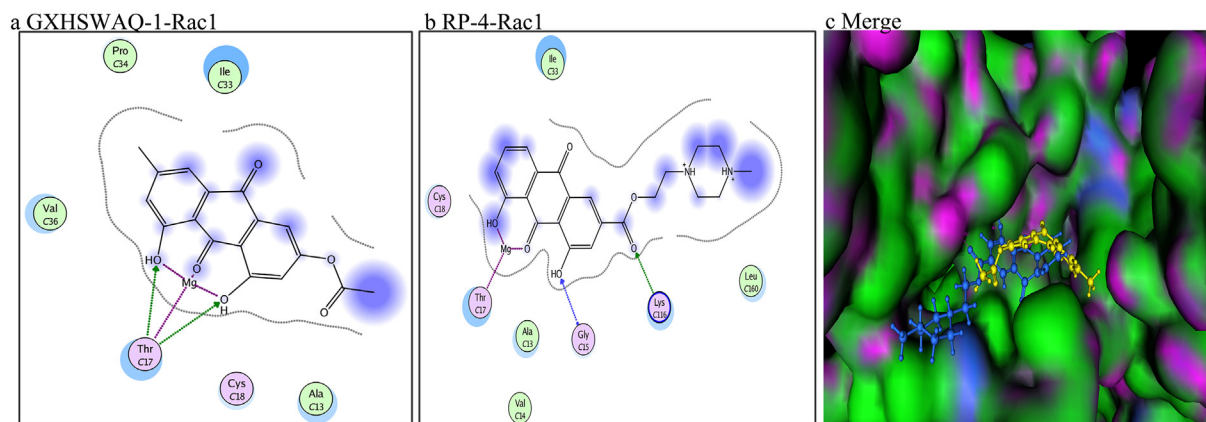


**Fig. 2.** View of the interaction modes of minimum energy conformation of GXHWSAQ-1 and RP-4 with Rac1. a) GXHWSAQ-1-Rac1 complex b) RP-4-Rac1 complex c) Superimposed view of the most dominant conformations of GXHWSAQ-1 and RP-4 in the binding pocket of Rac1. The sidechain hydrogen bond interactions were represented by green dotted arrows and backbone hydrogen bond interactions were represented by blue dotted arrows, purple dotted arrows indicated chelation interactions. The greasy residues were shown as green circles while polar residues were shown as pink circles. In picture c, the structure of RP-4 are shown with blue marked ball-stick model and GXHWSAQ-1 was marked with yellow. Purple indicates areas of hydrogen bond interaction, green and blue represents for hydrophobic regions and mild polar molecule regions, respectively. (For interpretation of the references to color in this figure legend, the reader is referred to the web version of this article.)

**Table 2**  
The inhibitory effect of RP4 on NPC CNE1 and CNE2 cells (n = 3,  $\bar{x} \pm s$ ).

Concentration ( $\mu\text{g}\cdot\text{mL}^{-1}$ )	Inhibition rate(%)	
	CNE1	CNE2
6.25	6.13 $\pm$ 1.52	15.74 $\pm$ 1.37
12.5	21.02 $\pm$ 1.67	30.77 $\pm$ 1.22
25	26.24 $\pm$ 1.33	37.32 $\pm$ 1.86
50	36.08 $\pm$ 1.55	55.74 $\pm$ 1.55
100	65.86 $\pm$ 1.43	59.83 $\pm$ 1.14

experimental results indicated that RP-4 decreased the survival rates of CNE1 and CNE2 cells in a concentration dependent way (Table 2). The half inhibition concentration (IC<sub>50</sub>) of RP-4 on CNE1 and CNE2 cells were 66.28  $\mu\text{g}\cdot\text{mL}^{-1}$  and 46.47  $\mu\text{g}\cdot\text{mL}^{-1}$ , respectively. 10% inhibition concentration (IC<sub>10</sub>) of RP-4 on CNE1 and CNE2 cells were 8.44  $\mu\text{g}\cdot\text{mL}^{-1}$  and 4.01  $\mu\text{g}\cdot\text{mL}^{-1}$ , which was observed to have no cytotoxic effects, therefore these concentrations were chosen for the subsequent experiments.

### 3.5. RP-4 induced the expression of active Rac1 GTPase increasing

Most reports have shown that the Rac1 GTPase was closely associated with the chemotherapy resistance of tumor cells [17]. Rac1 GTPases act as the molecular switches between the inactive GDP-Rac1 and the active GTP-Rac1 through which regulate varieties of signal transduction pathways and cellular function [18,19]. Based on our early findings, the mitochondrial target Rac1 protein was discovered to be closely associated with radiosensitization process, we further investigated whether the active Rac1 participated in the radiosensitization signaling pathways of nasopharyngeal carcinoma mediated by RP-4. The activation of Rac1 and total protein of Rac1 was separately determined by Rac1-GST pull-down assay and western blotting analysis. Here, we observed an obvious increasing expression of Rac1 in both CNE1 and CNE2 cells after the treatment with RP-4 compared with control, and simultaneously, a remarkable increasing of Rac1-GTP in CNE1 cells, while no prominent increase in CNE2 cells. GTP $\gamma$ S treatment trapped Rac1 in the GTP-bound, active form, resulting in a strong signal when endogenous Rac1 is present which was considered as positive control, while GDP treatment pushed Rac1 into the GDP-bound, inactive state, resulting in minimal or no signal. What's more, the combined treatment of RP-4 and irradiation could significantly increase the expression of both Rac1 and Rac1-GTP in the two cell lines relative to the treatment with irradiation alone (shown as Fig. 3).

### 3.6. The effects of RP-4 combined with radiotherapy on the activation of Rac1/NADPH signaling pathway in NPC CNE1 and CNE2 cells

To investigate whether Rac1/NADPH signaling pathway participated in the regulation of radiotherapy sensitization of nasopharyngeal carcinoma mediated by RP-4, the expression of two components of NADPH oxidase P47<sup>phox</sup> and P67<sup>phox</sup> were determined by Western blotting analysis. Results revealed that there existed no remarkable change on the expression of P47<sup>phox</sup> and P67<sup>phox</sup> in CNE1 and CNE2 cells after treatment with RP-4 in comparison with control. However, the combined application of RP-4 and irradiation could significantly up-regulated the expression of P47<sup>phox</sup> and P67<sup>phox</sup> in both CNE1 and CNE2 cells compared with the treatment with irradiation alone (shown as Fig. 4).

### 3.7. The effects of RP-4 on Rac1/NADPH signaling pathway in Rac1-overexpressed and Rac1-silenced cell lines

In order to verification whether Rac1 and Rac1/NADPH signaling

pathway were the direct targets of RP-4 in regulating radiosensitivity of NPC cell, Rac1 protein were separately knocked down and over-expressed in both CNE1 and CNE2 cells before treated with RP-4 under the concentration of IC<sub>50</sub>. Results suggested that the expression of Rac1, P47<sup>phox</sup> and P67<sup>phox</sup> were significantly upregulated in CNE1-Rac1(+) and CNE2-Rac1(+) cells after treated with RP-4, while no obvious differences were observed in CNE1-Rac1(-) and CNE2-Rac1(-) cells compared with the cells treated without RP-4. (shown as Fig. 5A-D).

### 3.8. The effects of the activated Rac1/NADPH on downstream JNK/AP-1 signaling pathway by the combined application of RP-4 and radiotherapy treatment in CNE1 and CNE2 cells

Anthony J. Valente etc. has reported that the ROS production induced by NADPH oxidase was able to regulate the activation of JNK/AP-1 [20]. Jun N-terminal Kinase (JNK) together with p38 belong to MAPK families, and the long time continuous activation of JNK are considered to associated with cell apoptosis [21]. Activator protein-1 (AP-1) is a downstream transcription factor in the MAPK pathway [22] and is also the major downstream target of JNK [23], involves in regulating adhesion molecule expression, its activation was dependent by Rac1/NADPH/ROS, which further promote the NADPH oxidases transcription [20]. Inspired by our discovery that RP-4 combined with irradiation could effectively activated Rac1/NADPH signaling pathway, we set about investigating the effects of the activation of Rac1/NADPH on the expression of the downstream related proteins of JNK/AP-1 signaling pathways. The expression level of these proteins including P38, phosphorylate-p38 (P-P38), AP-1, phosphorylate-AP-1 (P-AP-1), JNK1/2, and phosphorylate-JNK (P-JNK) in CNE1 and CNE2 cells after various treatments were determined by western blotting analysis. Our results showed that the treatment with RP-4 could significantly up-regulate the expression of P38, P-P38 and P-JNK (P < 0.05) but did not affect the expression of JNK1/2, Ap-1 or P-AP-1 in CNE1 cells compared with control (shown as Fig. 6A,B). In CNE2 cells, only an increased expression level of P38 was detected after the exposure of RP-4, besides, there were no significant effects on Ap-1, JNK1/2 or the expression of the phosphorylation of these three proteins (shown as Fig. 6C,D). While, the treatment of RP-4 combined with radiotherapy could significantly up-regulate the expression of P38 (P < 0.05), P-P38, P-AP-1 and P-JNK1/2 in both CNE1 and CNE2 cell lines compared with 2Gy group (P < 0.01). A stronger protein phosphorylation of JNK and AP-1 could be induced by RP-4 plus 2 Gy radiation.

### 3.9. The activated Rac1/NADPH affected the biological function of CNE1 and CNE2 cells by influencing NADPH oxidase activity and endogenous ROS production

It was reported that the small GTPase Rac1 participated in the activation of NADPH oxidase complex, thereby resulting in ROS production [9]. Having certified that the combined use of RP-4 and irradiation induced the activation of Rac1/NADPH and its downstream JNK/AP-1 signaling pathways, we further speculated whether the activation of this pathway directly affected the NADPH oxidase activity and endogenous ROS levels thereby leading to different influence on the biological function of CNE1 and CNE2 cells. Our result demonstrated that, the treatment of RP-4 under 10% inhibition concentration with CNE1 and CNE2 cells affected neither the NADPH oxidase activity nor the production of intracellular ROS relative to control, while the federated application of RP-4 and irradiation significantly increased both the NADPH oxidase activity and intracellular ROS level of the two cell lines compared with treated with irradiation alone (shown as Fig. 7). Besides, the ROS production induced by irradiation in the highly differentiated CNE1 cells after the treatments of RP-4 plus irradiation were more prominent compared with poorly differentiated CNE2 cells (see in Fig. 7 B).

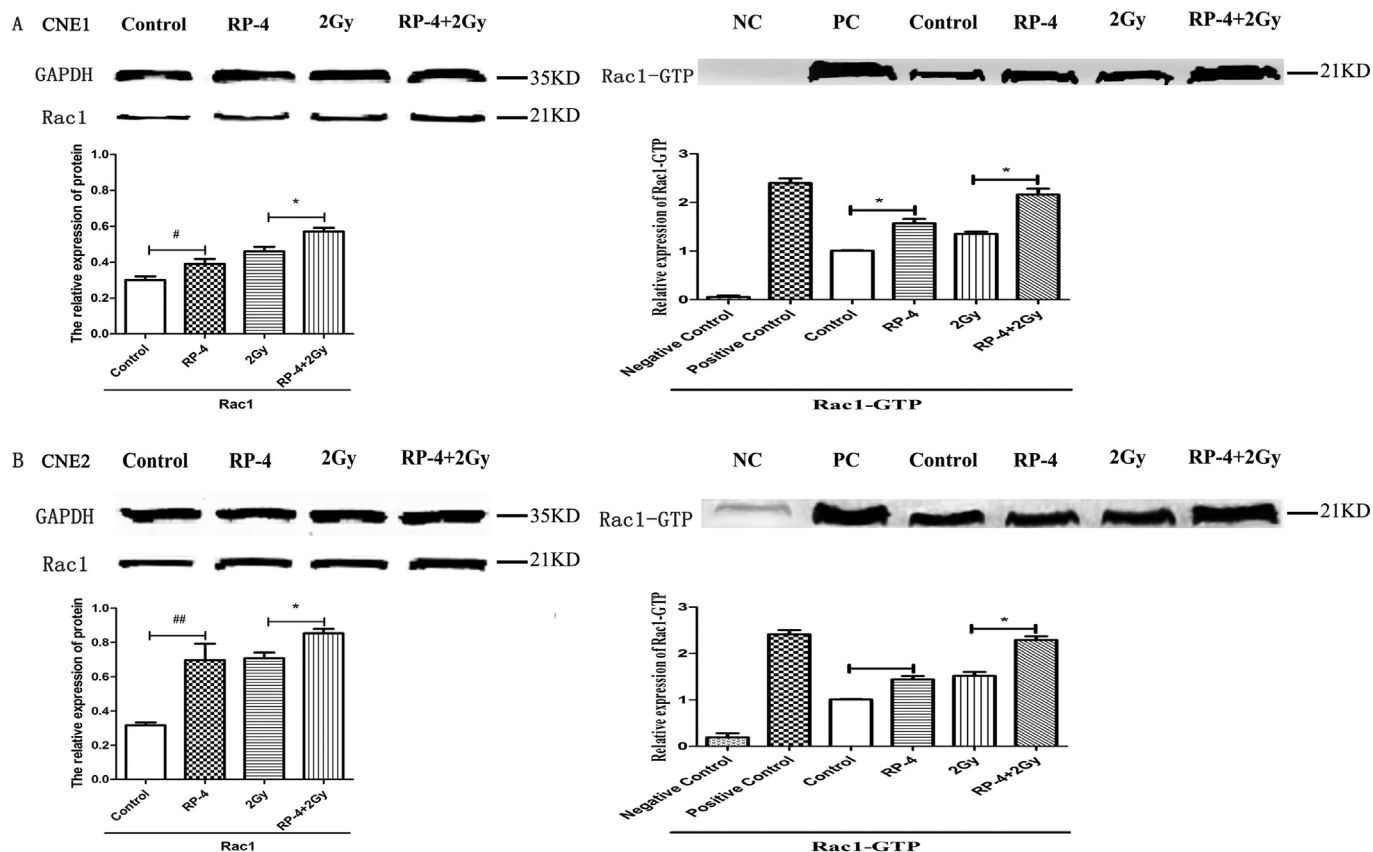


**Fig. 3.** The expression of Rac1 and Rac1-GTP in each group. After different treatments, the activation of Rac1 and total protein of Rac1 was separately determined by Rac1-GST pull-down assay and western blotting analysis. Pane A: CNE1 cell treated with RP-4, 2Gy alone, as well as with RP-4 and 2 Gy radiation. Pane B: CNE2 cell treated with RP-4, 2Gy alone, as well as with RP-4 and 2 Gy radiation. PC:positive control (GTPγS), NC: negative control (GDP). Data expressed as mean ± SD, n = 3. #P < 0.05, ## P < 0.01 compared with controls. \*P < 0.05, \*\*P < 0.01 compared with cells exposed to 2 Gy.

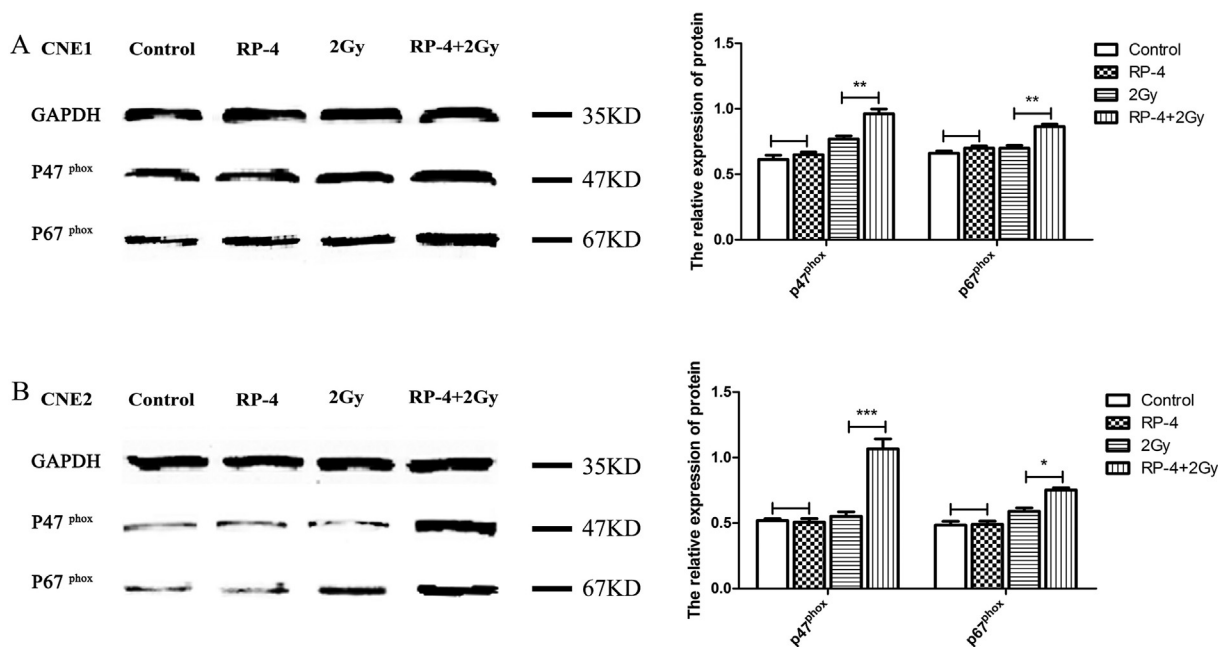


**Fig. 4.** The expression of P47<sup>phox</sup> and P67<sup>phox</sup> proteins in each group. After different treatments, Total cell lysates from samples were prepared for immunoblots to test GAPDH, P47<sup>phox</sup> and P67<sup>phox</sup> levels. Pane A: CNE1 cell treated with RP-4, 2Gy alone, as well as with RP-4 and 2 Gy radiation. Pane B: CNE2 cell treated with RP-4, 2Gy alone, as well as with RP-4 and 2 Gy radiation. Data represent mean ± SD, n = 3. \*P < 0.05, \*\*P < 0.01, \*\*\*P < 0.001 compared with cells exposed to 2 Gy.

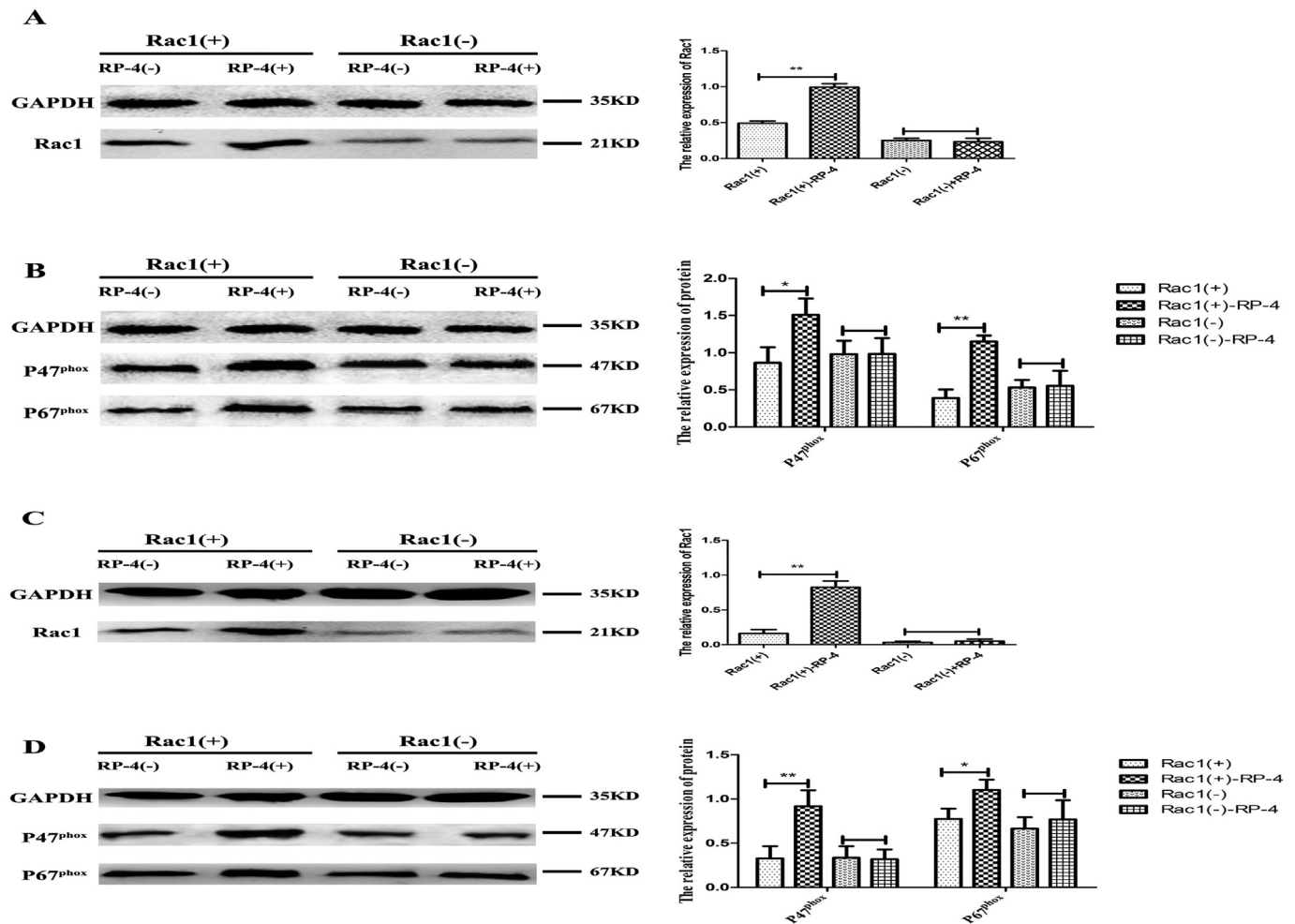


**Fig. 5.** The expression of Rac1/NADPH signaling pathway related proteins in Rac1 silenced and overexpressed cell lines treated with RP-4. A and B: Western blotting analysis of the Rac1/NADPH pathway in CNE1 cells treated with RP-4 after silenced and overexpressed Rac1. C and D: Western blotting analysis of the Rac1/NADPH pathway in CNE2 cells treated with RP-4 after silenced and overexpressed Rac1. GAPDH was used as a control for protein loading and integrity. N = 3. #P < 0.05 compared with Rac1-silenced cells treated without RP-4, \*P < 0.05, \*\*P < 0.01 compared with Rac1-overexpressed cells treated without RP-4.

### 3.10. The combined application of RP-4 and irradiation induced cell apoptosis

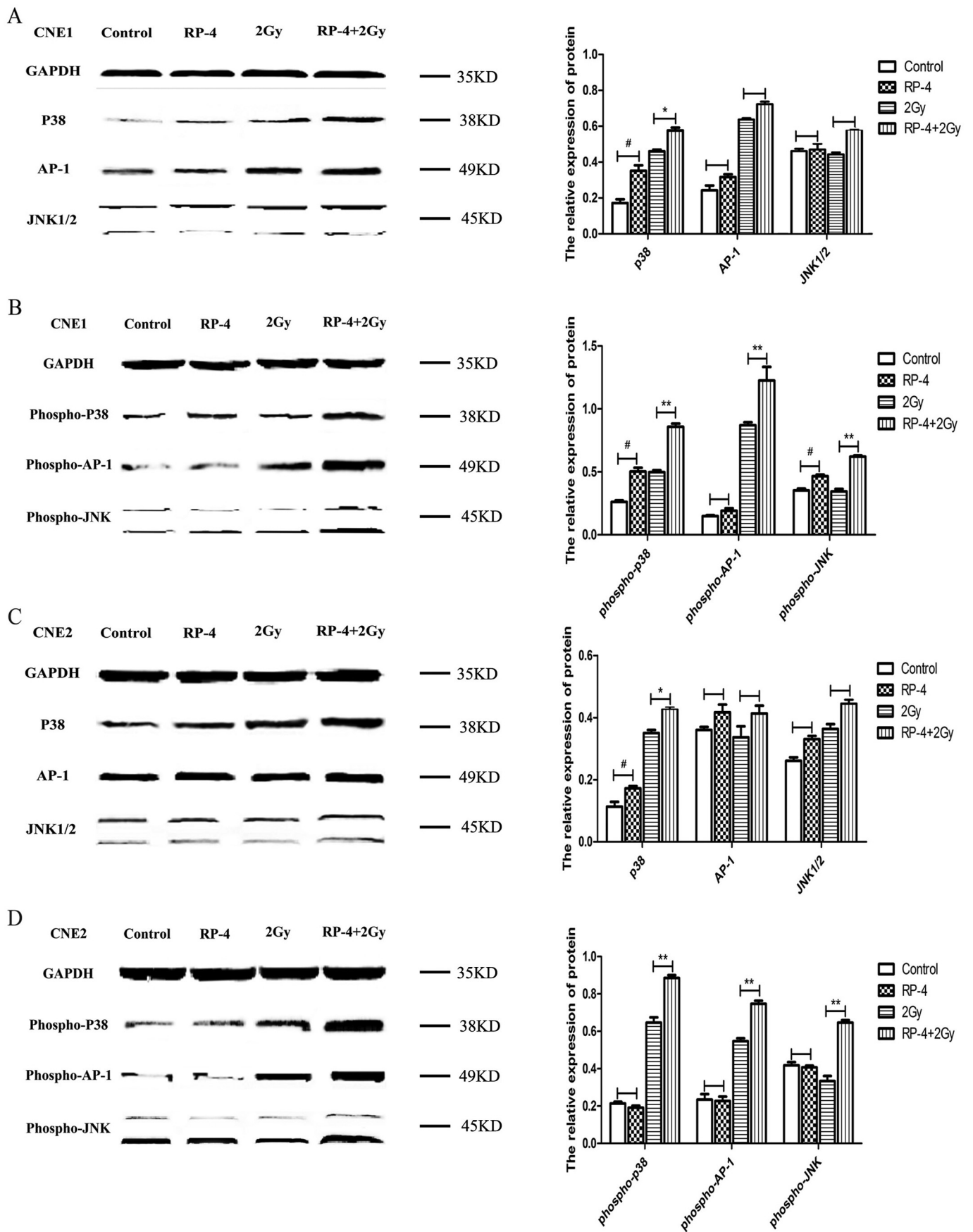
The induced generation of ROS production was considered to result in DNA damage followed by the apoptosis mediated by mitochondrial intrinsic pathways. Therefore, we detected the apoptosis rate of the cells after the activation of Rac1/NADPH pathway. Result showed that, the apoptosis rate of the cells was moderately increased after the cell were exposed to RP-4. In comparison, the apoptosis was significantly increased after dealt with the combined use of RP-4 and irradiation relative to the treatment of irradiation alone in CNE1 and CNE2 cells (shown as Fig. 8), which indicated that RP-4 was able to increase the radiation sensitivity of both CNE1 and CNE2 cells (Table 3).

## 4. Discussion

Drug discovery is hard and target medicine discovery is more difficult. Target medicine should in theory efficaciously attack pathogens but remain harmless in healthy tissue. Proper drug target selection and validation are crucial to the discovery of new drugs. According to our knowledge, the types of cancer tissues, microenvironment, and the body condition determined the radiosensitivity of tumors, which requires individualized treatments [24]. However, since there is no definite molecular targets responsible for radioresistance of cancer cells, no specifically selective radiosensitizer was discovered for clinical

application so far. It is necessary to perform preliminary research on identification of molecular targets responsible for radioresistance and focus on screening of various agents interacting with those targets. Rac1 GTPases act as the molecular switches between the inactive GDP-Rac1 and the active GTP-Rac1 through which regulate varieties of signal transduction pathways and cellular function. In our preliminary study, mass spectrum and bioinformatics analysis showed that Rac1 protein might be a mostly mitochondrial target in the radiosensitization process of nasopharyngeal carcinoma CNE1 cells. Activation of Rac1 is sufficient to induce NADPH oxidase production ROS increasing [25] and excessive ROS could trigger DNA damage and activate downstream signaling pathways to enhance the anticancer efficacy of radiation. Rac1 participated in the radiosensitization signaling pathways of nasopharyngeal carcinoma. In this study, we found the protein level of Rac1 in highly differentiated NPC CNE1 cell line was lower than poorly differentiated NPC CNE2 cell line. This may be why poorly differentiated human NPC CNE2 cell lines showed more sensitive to radiation than highly differentiated CNE1 cell lines [26]. Rac1 can serve as a predictive marker of the radiosensitization. And, furthermore, it can be used as a molecular target for designing and synthesizing more compounds to enhance the radiation response in radioresistant tumors.

In our previous work, the compound GXHWAQ-1 was synthesized from the nuclear structure of anthraquinone compound which showed a remarkable radiosensitization activity in nasopharyngeal carcinoma cells [5]. But the poor water solubility limited its development to a



(caption on next page)

**Fig. 6.** Western blotting analysis of the expression of JNK/AP-1 signaling pathway related proteins in CNE1 and CNE2 cells. A and C: The expression level of P38, AP-1 and JNK1/2 of CNE1 and CNE2 cells. B and D: The expression level of phospho-P38, phospho-AP-1 and phospho-JNK1/2 of CNE1 and CNE2 cells. GAPDH was used as a control for protein loading and integrity. The relative phosphorylated P38, AP-1 and JNK1/2 and total P38, AP-1 and JNK1/2 expression intensity from 3 samples was shown. #P < 0.05 compared with control, \*P < 0.05, \*\*P < 0.01 compared with cells exposed to 2 Gy.

clinical drug. Therefore, it is an urgent necessity to conduct a structural modification of GXHSAQ-1 to obtain an improved water solubility and enhanced radiosensitization activity. It was reported that the planar tricyclic structure of anthraquinone was essential for intercalating into DNA base pairs and exhibit significant DNA binding affinity thereby possessing remarkable cytostatic or cytotoxic activities [27]. Based on this guiding principle, the novel compound RP-4 was synthesized by preserved the planar tricyclic structure of anthraquinone. The side chain carboxyl site of anthraquinone compound Rhein participated in an esterification reaction with 1, 2-dibromoethane to form the carboxylic acid ester bridge chain, followed by introducing *N*-methyl piperazine groups to lead compound through nucleophilic substitution reaction (SN1). According to the liposome–water partition coefficients (expressed as LogP) of RP-4, Rhein and GXHSAQ-1 predicted by Chem Bio Draw Ultra, the introduction of the hydrophilic group *N*-methyl piperazine greatly improved water solubility of RP-4 compared with the lead compound GXHSAQ-1 and Rhein, which increased its possibility to be a clinical drug. Molecular docking of RP-4 toward the target protein Rac1 demonstrated that, the planar tricyclic structure of anthraquinone of RP-4 and GXHSAQ-1 could embedded in Rac1 hydrophobic pocket, which contributed a lot to improve the stability of the ligand and the receptor complexes. Additionally, the enhancement of the backbone hydrogen bond interactions with Rac1 promoted the binding affinity of RP-4 and Rac1. Therefore, the molecular docking results predicted a more favorable binding mode between RP-4 and Rac1. In this study, the expression of Rac1 was separately silenced and overexpressed by lentivirus transfection in both CNE1 and CNE2 cells. We found that Rac1 was significantly activated in CNE1-Rac1(+) and CNE2-Rac1(+) cells after treated with RP-4. However, the expression of Rac1 in CNE1-Rac1(–) and CNE2-Rac1(–) cells treated with RP-4 did not change after Rac1 silencing. The results of western blotting analysis and pull-down assay showed that RP-4 could effectively increase the Rac1 protein expression especially in CNE1 and CNE2 cells treated with RP-4 plus 2Gy irradiation. In addition, the results of viability experiment also showed that RP-4 inhibited the proliferation of nasopharyngeal carcinoma cells significantly. These results suggested that Rac1 serve as a potential pharmacological target of RP-4 for antitumor therapy in nasopharyngeal carcinoma.

It was reported that PMA was the activator of Rac1. We have found that the combined application of PMA and irradiation could effectively activate Rac1 which further regulated the activation of NADPH oxidase complex thereby resulting in ROS production and inducing CNE1 cell apoptosis [12]. Interesting note was that RP-4 plus irradiation could up-regulate Rac1 expression in both NPC CNE1 and CNE2 cells, but

whether or not RP-4 activated the same Rac1/NADPH signaling pathways to enhance radiosensitivity of NPC cells. Western blotting analysis results of two cell lines demonstrated that treatment of RP-4 alone had little effects on Rac1/NADPH pathway, but the combined treatment of RP-4 and irradiation with NPC cells could effectively up-regulated the expression of two mainly subunits of NADPH, P47<sup>phox</sup> and P67<sup>phox</sup>. Also we identified an remarkable enhancement of NADPH oxidase activity and ROS production as well as an increasing cell apoptosis rate. What's more, Rac1/NADPH signaling pathway were significantly activated in Rac1-overexpressed CNE1 and CNE2 cells after treated with RP-4. While, after silencing Rac1 no obvious effects of RP-4 on the expression of Rac1, P47<sup>phox</sup> and P67<sup>phox</sup> were observed. These results provide strong evidence that Rac1 and NADPH oxidase may probably be the direct targets of RP-4 in regulating radiosensitivity of NPC cells.

There is substantial evidence showing that the ROS produced by Rac1/NADPH pathway could activated downstream JNK/AP-1 signal pathway, which consist of c-jun N-terminal kinases (JNKs), AP-1 and the p38 kinase [28]. JNK/AP-1 signal pathway mediated by ROS are involved in cell growth, differentiation and apoptosis [29]. Its activation mainly is regulated by the post-translational modifications, the level of phosphorylation of c-jun controls the activities of transcript and DNA binding of AP-1 [30]. It has been reported that AP-1 could be activated and phosphorylated at the N-terminal region of the c-jun by JNK, a member of the MAPK family [31]. Similar to the properties of JNK, p38 kinase is activated by a variety of cellular stresses including UV irradiation, HSP, Rac1 and so on. P38 kinase are activated by MAPK kinases-mediated dual Threonine and Tyrosine phosphorylation. These residues phosphorylated during activation are Thr183/Tyr185 of JNK and Thr180/Tyr182 of p38 MAPK [32]. Persistent activation of JNK and P38 could result in phosphorylation of serine residues at the amino end of transcription factor c-Jun, which binds to the promoter region of AP-1, increase the transcriptional activation of AP-1, induced cells autophagy and apoptosis [33,34]. The present study found that the activated Rac1/NADPH pathway induced by RP-4 and irradiation could significantly up-regulate the expression of P38, AP-1, JNK1/2 and effects on phosphorylation of those proteins in NPC cells. As shown in Fig. 5, RP-4 alone could significantly up-regulate the expression of P38 and P-P38, but did not affect the expression of JNK1/2 and Ap-1 in NPC cells compared with control. When RP-4 plus 2Gy treatment, the activities of AP-1 and the expression of P-JNK1/2 and P-P38 were remarkably increased compared with 2Gy group. Our results suggest that RP-4 could up-regulate Rac1, cooperatively activate JNK and P38, cause NPC radiosensitization may probably by regulating the Rac1/NADPH/JNK/AP-1 signaling axis. These results confirmed the role of

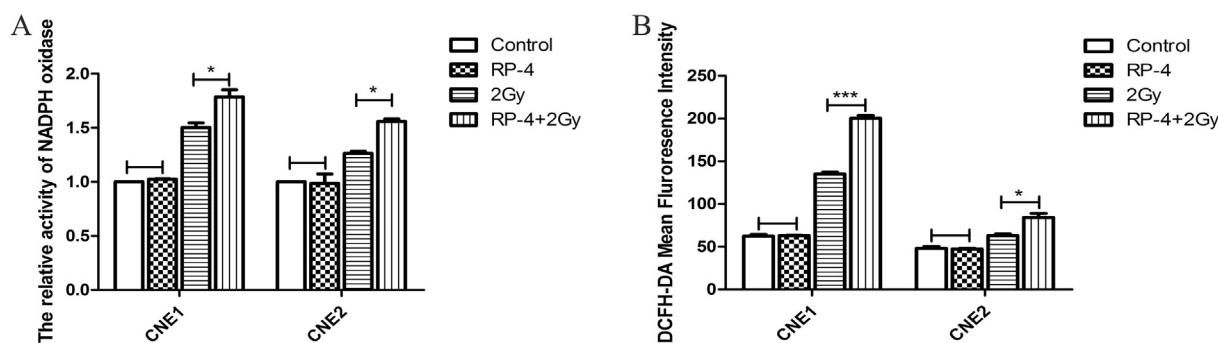


**Fig. 7.** The measurement of NADPH oxidase activity and concentration of ROS in CNE1 and CNE2 cells. A: NADPH oxidase activity of each group of cells was measured by nitroblue tetrazolium assay, which was expressed as the percentage of absorbance relative to control. B: ROS production of the cells analyzed by flow cytometry technology was shown as fluorescence intensity. \*P < 0.05, \*\*P < 0.01, \*\*\*P < 0.001 compared with cells exposed to 2 Gy.

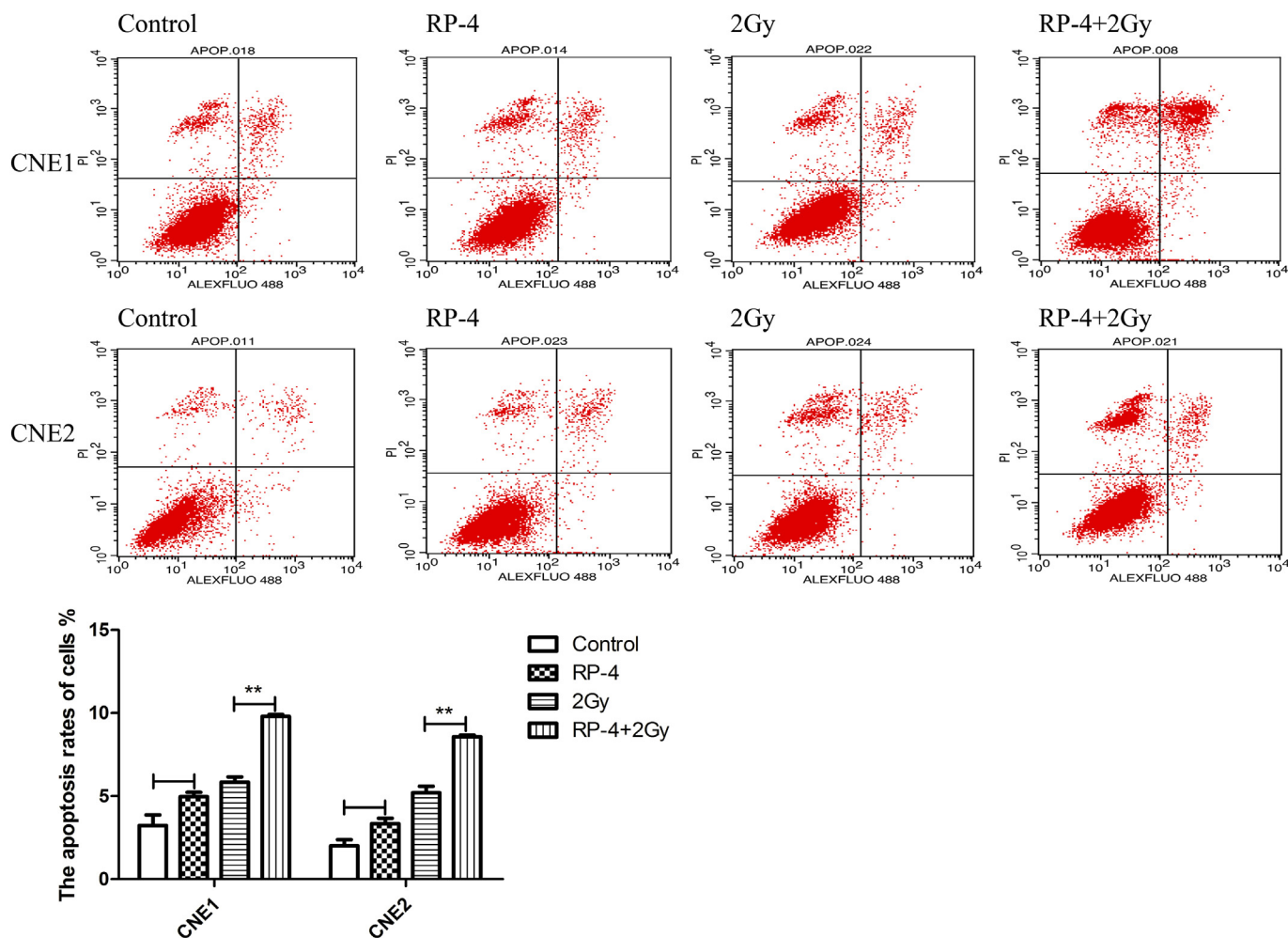


Fig. 8. The apoptosis rate of each group.

Table 3  
The apoptosis rate of each group.

	Control	RP-4	2Gy	RP-4 + 2Gy
CNE1	3.23 ± 0.64	4.97 ± 0.26	5.85 ± 0.31	9.79 ± 0.12*
CNE2	2.01 ± 0.37	3.35 ± 0.32	5.21 ± 0.39	8.58 ± 0.10*

\* P < 0.01 compared with 2Gy.

Rac1 target protein and also demonstrated the mechanism of RP-4 as a potential radiosensitizer.

In summary, we reported the important roles of Rac1/NADPH/JNK/AP-1 signaling pathway in mediating radiosensitivity in differently differentiated NPC cell models. According to the results, new compound RP-4 could effectively modulate NPC radiosensitization as a potential radiosensitizer. We also confirmed the role of Rac1 target protein in modulating the NPC radiosensitization. We believed our results would provide new strategies for the development design of radiotherapy sensitization agent with an anthraquinone nucleus structure and identify the possibility of Rac1 protein to be a potential target for the radiotherapy treatment.

**Conflicts of interest**

The authors of this manuscript have no potential conflicts of interest to declare.

**Acknowledgments**

This study was supported by grants obtained from the National Natural Science Foundation of China (No. 81460561, No. 81360502) and Guangxi Natural Science Foundation (No. 2014GXNSFAA118225).

**References**

- [1] G. Luo, Y. Zhou, W. Yi, H. Yi, Expression levels of JNK associated with polymorphic lactotransferrin haplotypes in human nasopharyngeal carcinoma, *Oncol. Lett.* 12 (2) (2016) 1085–1094.
- [2] C.Y. Huang, W.T. Tai, S.Y. Wu, C.T. Shih, M.H. Chen, M.H. Tsai, C.W. Kuo, C.W. Shiau, M.H. Hung, K.F. Chen, Dovitinib Acts as a Novel Radiosensitizer in Hepatocellular Carcinoma by Targeting SHP-1/STAT3 Signaling, *Int. J. Radiat. Oncol. Biol. Phys.* 95 (2) (2016) 761–771.
- [3] L. Peterk, P.H.C. Chan, David C. Frost, Brian R. James, Ruthenium (II) complexes of 4-nitroimidazoles their characterization, solution chemistry, and radiosensitizing activity, *Can. J. Chem.* 66 (1988) 117–122.
- [4] X. Sun, C. Yang, H. Liu, Q. Wang, S.X. Wu, X. Li, T. Xie, K.L. Brinkman, B.S. Teh, E.B. Butler, B. Xu, S. Zheng, Identification and characterization of a small inhibitory peptide that can target DNA-PKcs autophosphorylation and increase tumor radiosensitivity, *Int. J. Radiat. Oncol. Biol. Phys.* 84 (5) (2012) 1212–1219.
- [5] Y. Mo, H. Hou, D. Li, Y. Liang, D. Chen, Y. Zhou, Mitochondrial protein targets of radiosensitisation by 1,8-dihydroxy-3-acetyl-6-methyl-9,10 anthraquinone on nasopharyngeal carcinoma cells, *Eur. J. Pharmacol.* 738 (2014) 133–141.
- [6] Z. Su, W. Tian, J. Li, C. Wang, Z. Pan, D. Li, H. Hou, Biological evaluation and molecular docking of Rhein as a multi-targeted radiotherapy sensitization agent of nasopharyngeal carcinoma, *J. Mol. Struct.* 1147 (2017) 462–468.
- [7] James C. Mulloy, J.A.C. Marie-Dominique Filippi, Theodosia A. Kalfa, Fukun Guo, Yi Zheng, Rho GTPases in hematopoiesis and hemopathies, *Blood* 115 (5) (2010) 936–947.
- [8] S. Chen, H. Li, S. Li, J. Yu, M. Wang, H. Xing, K. Tang, Z. Tian, Q. Rao, J. Wang, Rac1 GTPase Promotes Interaction of Hematopoietic Stem/Progenitor Cell with

- Niche and Participates in Leukemia Initiation and Maintenance in Mouse, *Stem Cells* 34 (7) (2016) 1730–1741.
- [9] R. Velaithan, J. Kang, J.L. Hirpara, T. Loh, B.C. Goh, M. Le Bras, C. Brenner, M.V. Clement, S. Pervaiz, The small GTPase Rac1 is a novel binding partner of Bcl-2 and stabilizes its antiapoptotic activity, *Blood* 117 (23) (2011) 6214–6226.
- [10] G. den Hartog, R. Chattopadhyay, A. Ablack, E.H. Hall, L.D. Butcher, A. Bhattacharyya, L. Eckmann, P.R. Harris, S. Das, P.B. Ernst, S.E. Crowe, Regulation of Rac1 and reactive oxygen species production in response to infection of gastrointestinal epithelia, *PLoS Pathog.* 12 (1) (2016) 1–20.
- [11] I. Bahar, G. Elay, G. Başkol, M. Sungur, H. Donmezaltuntas, Increased DNA damage and increased apoptosis and necrosis in patients with severe sepsis and septic shock, *J. Crit. Care* 43 (2018) 271–275.
- [12] C. Wang, Z. Pan, H. Hou, D. Li, Y. Mo, C. Mo, J. Li, The enhancement of radiation sensitivity in nasopharyngeal carcinoma cells via activation of the Rac1/NADPH signaling pathway, *Radiat. Res.* 185 (6) (2016) 638–646.
- [13] A. Wadood, M. Riaz, S.B. Jamal, M. Shah, Interactions of ketoamide inhibitors on HCV NS3/4A protease target: molecular docking studies, *Mol. Biol. Rep.* 41 (1) (2014) 337–345.
- [14] R.I. Al-Wabli, M.A. Khedr, A.A. Kadi, M.A. Motaleb, K.A. Al-Rashood, W.A. Zagahary, Synthesis, molecular docking and antibacterial evaluation of various quinoline schiff bases: labeling and biodistribution of <sup>99m</sup>Tc-2-(p-hydroxybenzylidene)-1-(quinolin-4-yl) hydrazine, *Med. Chem. Res.* 23 (9) (2014) 4011–4020.
- [15] A. Wadood, S.B. Jamal, M. Riaz, A. Mir, Computational analysis of benzofuran-2-carboxylic acids as potent Pim-1 kinase inhibitors, *Pharm. Biol.* 52 (9) (2014) 1170–1178.
- [16] N. Ferri, Corsini Alberto, Bottino Paolo, Clerici Francesca, Contini Alessandro, Virtual screening approach for the identification of new Rac1 inhibitors, *J. Med. Chem.* 52 (14) (2009) 4087–4090.
- [17] J.-Y. Wang, P. Yu, S. Chen, H. Xing, Y. Chen, M. Wang, K. Tang, Z. Tian, Q. Rao, J. Wang, Activation of Rac1 GTPase promotes leukemia cell chemotherapy resistance, quiescence and niche interaction, *Mol. Oncol.* 7 (5) (2013) 907–916.
- [18] M. Norbert Maggi, Patrizio Arrigo IEEEE, Carmelina Ruggiero, Member, IEEEE, Comparative Analysis of Rac1 Binding Efficiency With Different Classes of Ligands: Morpholines, Flavonoids, Imidazoles, *IEEE Trans. Nanobiosci.* 11 (2) (2012) 181–187.
- [19] T.Y. Prudnikova, S.J. Rawat, J. Chernoff, Molecular pathways: targeting the kinase effectors of RHO-family GTPases, *Clin. Cancer Res.* 21 (1) (2015) 24–29.
- [20] A.J. Valente, T. Yoshida, R. Izadpanah, P. Delafontaine, U. Siebenlist, B. Chandrasekar, Interleukin-18 enhances IL-18R/Nox1 binding, and mediates TRAF3IP2-dependent smooth muscle cell migration. Inhibition by simvastatin, *Cell. Signal.* 25 (6) (2013) 1447–1456.
- [21] J. Shi, C. Zhang, Z. Yi, C. Lan, Explore the variation of MMP3, JNK, p38 MAPKs, and autophagy at the early stage of osteoarthritis, *IUBMB Life* 68 (4) (2016) 293–302.
- [22] J.K. Li, L. Nie, Y.P. Zhao, Y.Q. Zhang, X. Wang, S.S. Wang, Y. Liu, H. Zhao, L. Cheng, IL-17 mediates inflammatory reactions via p38/c-Fos and JNK/c-Jun activation in an AP-1-dependent manner in human nucleus pulposus cells, *J. Transl. Med.* 14 (77) (2016) 1–10.
- [23] X. Li, Q. Liang, W. Liu, N. Zhang, L. Xu, X. Zhang, J. Zhang, J.J. Sung, J. Yu, Ras association domain family member 10 suppresses gastric cancer growth by co-operating with GSTP1 to regulate JNK/c-Jun/AP-1 pathway, *Oncogene* 35 (19) (2016) 2453–2464.
- [24] J. Pan, L. Zang, Y. Zhang, J. Hong, Y. Yao, C. Zou, L. Zhang, Y. Chen, Early changes in apparent diffusion coefficients predict radiosensitivity of human nasopharyngeal carcinoma xenografts, *Laryngoscope* 122 (4) (2012) 839–843.
- [25] P.L. Hordijk, Regulation of NADPH oxidases: the role of Rac proteins, *Circ. Res.* 98 (4) (2006) 453–462.
- [26] Z.Y. Xiao Bao, Siyang Wang, Yujia Zheng, Mingwei Wang, Bingxin Gu, Jianping Zhang, Yongping Zhang, C. Zhang, The preclinical study of predicting radiosensitivity in human nasopharyngeal carcinoma xenografts by 18F-ML-10 animalPET/CT imaging, *Oncotarget* 7 (15) (2016) 20743–20752.
- [27] L.W. Hsin, H.P. Wang, P.H. Kao, O. Lee, W.R. Chen, H.W. Chen, J.H. Guh, Y.L. Chan, C.P. His, M.S. Yang, T.K. Li, C.H. Lee, Synthesis, DNA binding, and cytotoxicity of 1,4-bis(2-amino-ethylamino)anthraquinone-amino acid conjugates, *Bioorg. Med. Chem.* 16 (2) (2008) 1006–1014.
- [28] S. Yadav, N. Kalra, L. Ganju, M. Singh, Activator protein-1 (AP-1): a bridge between life and death in lung epithelial (A549) cells under hypoxia, *Mol. Cell. Biochem.* 5 (1–12) (2017).
- [29] C.B. Ahn, W.K. Jung, S.J. Park, Y.T. Kim, W.S. Kim, J.Y. Je, Gallic acid-g-chitosan modulates inflammatory responses in LPS-stimulated RAW264.7 cells via NF-kappaB, AP-1, and MAPK pathways, *Inflammation* 39 (1) (2016) 366–374.
- [30] H. Wang, Z.C. Tu, G.X. Liu, L. Zhang, Y. Chen, Identification and quantification of the phosphorylated ovalbumin by high resolution mass spectrometry under dry-heating treatment, *Food Chem.* 210 (2016) 141–147.
- [31] X.-M. Li, S. Wu, T. Shi, H.-J. Fan, D.-Z. Li, Study on JNK/AP-1 signaling pathway of airway mucus hypersecretion of severe pneumonia under RSV infection, *Eur. Rev. Med. Pharmacol. Sci.* 20 (2016) 853–857.
- [32] K. Saeki, N. Kobayashi, Y. Inazawa, H. Zhang, H. Nishitoh, H. Ichijo, K. Saeki, M. Isemura, A. Yuo, Oxidation-triggered c-Jun N-terminal kinase (JNK) and p38 mitogen-activated protein (MAP) kinase pathways for apoptosis in human leukaemic cells stimulated by epigallocatechin-3-gallate (EGCG): a distinct pathway from those of chemically induced and receptor, *Biochem. J.* 368 (Pt 3) (2002) 705.
- [33] S. Fittipaldi, N. Mercatelli, I. Dimauro, M.J. Jackson, P.M. Paola, D. Caporossi, Alpha B-crystallin induction in skeletal muscle cells under redox imbalance is mediated by a JNK-dependent regulatory mechanism, *Free Radic. Biol. Med.* 86 (2015) 331–342.
- [34] V.M. Campa, J.M. Iglesias, M.T. Carcedo, R. Rodríguez, J. Riera, S. Ramos, P.S. Lazo, Polyinosinic acid induces TNF and NO production as well as NF-κB and AP-1 transcriptional activation in the monocytemacrophage cell line RAW 264.7, *Inflamm. Res.* 54 (8) (2005) 328.